NANO LETTERS

Letter

pubs.acs.org/NanoLett

A Double-Strip Plasmonic Waveguide Coupled to an Electrically Driven Nanowire LED

You-Shin No,[†] Jae-Hyuck Choi,[†] Ho-Seok Ee,[†] Min-Soo Hwang,[†] Kwang-Yong Jeong,[†] Eun-Khwang Lee,[‡] Min-Kyo Seo,[‡] Soon-Hong Kwon,[§] and Hong-Gyu Park*[,†]

[†]Department of Physics, Korea University, Seoul 136-701, Republic of Korea

[‡]Department of Physics and Institute for the NanoCentury, KAIST, Daejeon 305-701, Republic of Korea

[§]Department of Physics, Chung-Ang University, Seoul 156-756, Republic of Korea

Supporting Information

ABSTRACT: We demonstrate the efficient integration of an electrically driven nanowire (NW) light source with a double-strip plasmonic waveguide. A top-down-fabricated GaAs NW light-emitting diode (LED) is placed between two straight gold strip waveguides with the gap distance decreasing to 30 nm at the end of the waveguide and operated by current injection through the p-contact electrode acting as a plasmonic waveguide. Measurements of polarization-resolved images and spectra show that the light emission from the NW LED was coupled to a plasmonic waveguide mode, propagated through the waveguide, and was focused onto a subwavelength-sized spot of surface plasmon polaritons at the tapered end of the waveguide. Numerical simulation agreed well with these experimental results, confirming that a symmetric plasmonic waveguide mode was excited on the top surface of the waveguide. Our demonstration of a plasmonic waveguide coupled to an electrically driven NW LED represents important progress toward further miniaturization and practical implementation of ultracompact photonic integrated circuits.

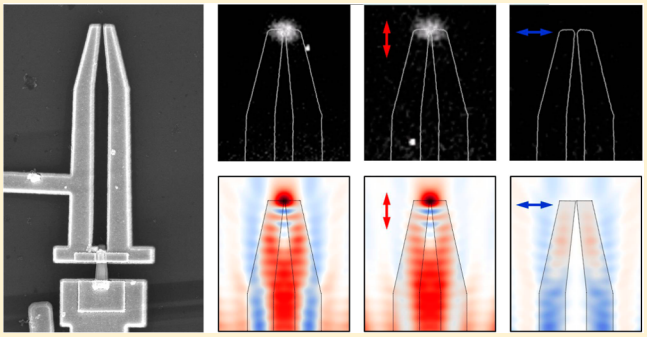

KEYWORDS: *Surface plasmon polaritons, semiconductor nanowires, light-emitting diodes, plasmonic waveguides, FDTD simulations, photonic integrated circuits*

Plasmonic devices such as plasmonic waveguides and lasers enable efficient light manipulation using surface plasmon polaritons (SPPs) in a subwavelength regime.[1−14] Various plasmonic waveguides have been intensively investigated as essential components in ultracompact plasmonic integrated circuits. For example, waveguiding and the subwavelength cross-sectional confinement of SPPs were successfully demonstrated using the metallic nanostrips,[9,10] V-shaped grooves,[11,12] and slot plasmonic waveguides.[13,14] Although the key features of these plasmonic waveguides have been well-characterized, bulky external light sources must still be used to inject photons or SPPs into such subwavelength-scale waveguides.[15−17] Recently, nanoscale incoherent light sources were fabricated using semiconductor nanowires (NWs) and combined with plasmonic waveguides for the generation of SPPs.[18] However, efforts for the efficient integration of nanoscale internal light sources with plasmonic waveguides on a chip scale and the functionality of plasmonic devices have not been widely explored. In this Letter, we demonstrate a plasmonic waveguide coupled to an electrically driven NW light-emitting diode (LED) and observe the propagation of SPPs through the plasmonic waveguide. In addition, we measure the focusing of SPPs onto a subwavelength-scale spot at the end of the waveguide, which could be useful for constructing on-chip integrated photonic devices for biochemical sensing and quantum information requiring strong light−matter interactions.[19,20]

Our plasmonic structure consists of a semiconductor NW LED and a double-strip metallic waveguide (Figure 1A). The NW LED with an axial p/n junction is aligned to the central axis of the double-strip waveguide, and two gold contacts are connected to both p- and n-doped ends of the NW to inject current. The waveguide structure acts as p-contact electrode and also couples the electroluminescence (EL) emission from the NW LED to an SPP waveguide mode. The gap and width of the double-strip plasmonic waveguide gradually decrease from one end to the other, to focus the guided SPPs into a small spot.[19] Figure 1B shows an SEM image of the fabricated structure in which the NW LED is integrated with the double-strip gold waveguide on SiO_2 substrate. The length and width of one straight gold strip are 8.5 and 1.0 μm, respectively, and the gap between the two strips gradually decreases from 800 to

Received: December 5, 2012
Revised: December 25, 2012
Published: January 16, 2013

   dx.doi.org/10.1021/nl3044822 | *Nano Lett.* 2013, 13, 772−776

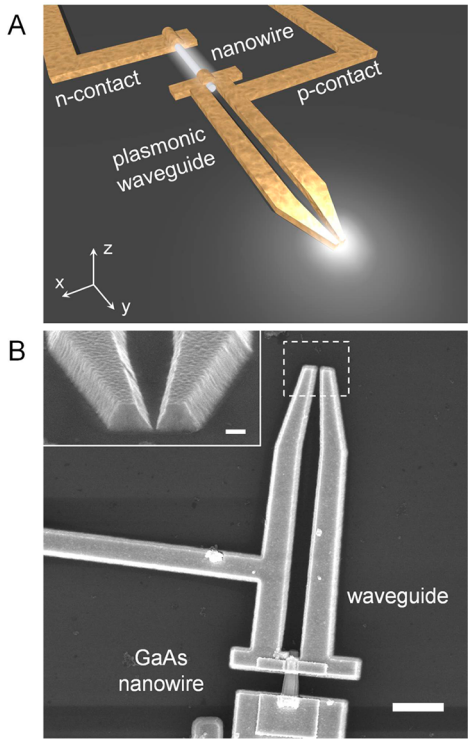

Figure 1. (A) Schematic illustration of a double-strip plasmonic waveguide coupled to an electrically driven GaAs NW LED. (B) SEM image of the fabricated structure. A GaAs NW with an axial p/n junction was used as an internal light source and integrated with the double-strip gold waveguide. The scale bar is 2 μm. The inset shows the tilted view of the tapered section of the waveguide, indicated by the white dotted square. The gold strip has a trapezoidal cross section. The scale bar in the inset is 300 nm.

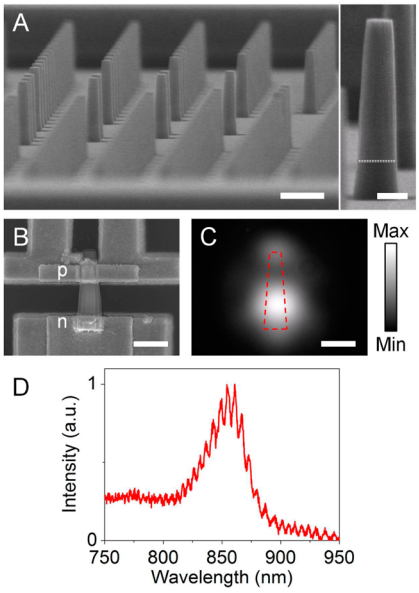

Figure 2. Fabrication and optical properties of a GaAs NW LED. (A) SEM image of vertical arrays of the NWs fabricated by EBL and dry etching. The scale bar is 2 μm. The right panel shows the magnified SEM image of a triangular cross-sectional single NW with a length of ~2.3 μm. The white dotted line indicates the sonication cleavage interface to separate NWs from the substrate. The scale bar is 500 nm. (B) SEM image of the fabricated NW LED. The scale bar is 1 μm. (C) EL image of the NW LED captured by a CCD camera. The NW in (B) was superimposed on the image as the red dotted line. The scale bar is 1 μm. (D) Measured EL spectrum from the NW LED. A current pulse with a peak value of 22.4 μA and a 10% duty cycle was injected.

30 nm along the 3.5 μm long tapered section (inset of Figure 1B). The width of one strip in the tapered section also decreases linearly from 1000 to 600 nm. These structural parameters were measured at the bottom surface of the waveguide. The smooth transition in the tapered section of the waveguide can minimize the scattering loss of SPPs, and therefore, the subwavelength-sized focusing of SPPs can be achieved efficiently.[21,22]

The electrically driven NW LEDs were fabricated using epitaxially grown p/n GaAs wafer (see Methods in Supporting Information). Triangular-shaped poly(methyl methacrylate) (PMMA) patterns were defined using electron-beam lithography (EBL), and chemically assisted ion beam etching (CAIBE) was applied using the patterns as a mask. Arrays of vertical NWs with a triangular cross section and a length of 2.3 μm were then formed (Figure 2A). One side of the triangular cross-section changes linearly from 400 to 700 nm along the NW axis as a result of the dry etching. The vertically etched NWs were submerged in ethanol solution and sonicated to isolate the NWs from the bottom substrate. Since the material composition of the etched NWs was abruptly changed at the interface of the bottom end of the NW (white dotted line, right panel of Figure 2A), the NWs were broken selectively at the interface. We dispersed these NWs on SiO_2 receiving substrate and fabricated p- and n-contacts and the double-strip waveguide through aligned EBL and deposition of chromium and gold layers (Figure S1). Figure 2B shows an SEM image of the fabricated NW LED. The conformal deposition of metal contacts was achieved due to the triangular cross section of the NW. In addition, since the plasmonic waveguide functions as the p-contact electrode of the NW LED, a simplified fabrication procedure and high yields were achieved in the integration of the NW internal light source with the plasmonic waveguide. This distinguishes our plasmonic structure from the previously reported ones that require significant modification of the structural design to couple SPPs to the waveguides.[15−17]

The optical properties of the fabricated GaAs NW LED were characterized by measurements of the EL images and spectra. The NW LED was electrically pumped by using 100 ns current pulses at a repetition rate of 1 MHz at room temperature. The light emitted from the NW LED was collected by a ×50 long-working-distance microscope objective lens focused onto either a spectrometer or a thermoelectrically cooled charge-coupled device (CCD) camera. Figure 2C shows the EL image from the NW LED, which was captured by the CCD camera. The light emission was clearly observed over the whole NW, except for the region where the electrical contacts blocked the EL emission from the NW LED. The EL spectrum shows multiple resonant peaks (Figure 2D). The peaks correspond to the Fabry−Perot oscillations of the fundamental and higher-order guided modes in the NW cavity.[23,24] It is known that several transverse modes can also be excited in each longitudinal mode in a triangular cross-sectional NW cavity with one side length of a few hundred nanometers.[25] In addition, to further investigate the optical and electrical properties of the NW LEDs, we measured EL spectra as a function of current, polarization state, and current versus voltage curve (Figure S2).

To examine how the EL emission from the NW LED is coupled into and propagates through the plasmonic waveguide,

dx.doi.org/10.1021/nl3044822 | Nano Lett. 2013, 13, 772−776

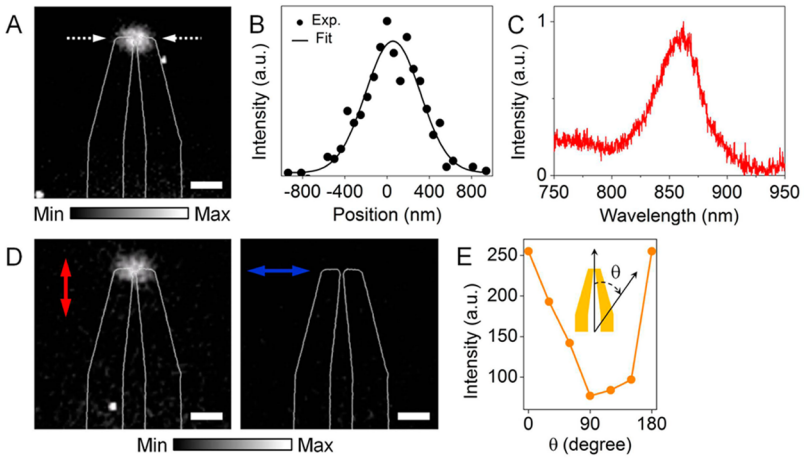

Figure 3. Measurement of the scattered light intensity at the tapered end of the double-strip plasmonic waveguide. (A) Measured CCD image of the light intensity distribution. A current pulse with a peak value of 22.4 μA and a 10% duty cycle was injected into the NW LED. The contour line of the waveguide obtained from the SEM image of Figure 1B was superimposed on the image. The scale bar is 1 μm. (B) Line scan through the CCD image in (A) taken along the white dotted arrows. The position in the *x*-axis was measured from the gap center of the waveguide. The black line is a Gaussian fit to the measured data (black dots). (C) Emission spectrum at the end of the waveguide. The light from the region covering the white dotted square in Figure 1B was integrated. (D) Polarization-resolved images of (A). A linear polarizer with the polarization direction parallel (left) or perpendicular (right) to the waveguide axis was placed in front of the CCD camera and spectrometer. The scale bar is 1 μm. (E) The intensity of the focused light spot was plotted as a function of the angle, θ, between the waveguide axis and the direction of the linear polarizer.

we measured the scattered light intensity distributions from the waveguide. A current pulse with a peak value of 22.4 μA and a 10% duty cycle was injected into the NW LED. Measurements showed that the light coupled from the NW LED to the double-strip plasmonic waveguide propagated without scattering along the waveguide with a total length of ~12 μm. The guided SPPs were then strongly focused onto a submicrometer-sized spot at the end of the waveguide (Figure 3A). To estimate accurately the size of the focused spot, the line scan through this measured image, taken along the white dotted arrows shown in Figure 3A, was plotted as a function of the position from the gap center of the waveguide (Figure 3B). This plot shows that the scattered light was localized within a subwavelength-scale spot with a size of ~600 nm full width at half-maximum (fwhm). The spot size will be smaller in near-field measurements.[19,20] In addition, we measured the spectrum of the focused light spot (Figure 3C), in which the central wavelength and spectral width are almost identical to those of the NW LED in Figure 2D.

Next, we measured polarization-resolved images and spectra of the scattered light intensity from the waveguide by rotating a linear polarizer in front of the CCD camera and spectrometer. The focused light spot was clearly observed in the polarization direction along the waveguide axis (left, Figure 3D), while the scattered light was not observed in the polarization direction perpendicular to the waveguide axis (right, Figure 3D). These results are summarized in the graph of the scattered light intensity, which is plotted as a function of the polarization angle θ relative to the waveguide axis (Figure 3E). The fact that the signal was predominantly polarized along the waveguide axis indicates that the scattered light originated from an SPP waveguide mode with a specific polarization direction. Taken together, the double-strip plasmonic waveguide effectively manipulated the light coupled from the NW LED and generated a subwavelength-sized focused light emission pattern.

To further investigate the optical properties of the guided SPP modes in the double-strip plasmonic waveguide, we calculated their dispersion curves and intensity profiles using finite-difference time-domain (FDTD) simulation. In particular, we can identify which SPP waveguide mode was excited in experiment by performing the simulations in the same waveguide structure as the one fabricated in Figure 1B. First, the two straight gold strips with a trapezoidal cross section were introduced on SiO_2 substrate while maintaining an air gap of 30 nm between the strips. The thickness and bottom width of one strip were set to 400 and 600 nm, respectively. A dipole emitter with a wavelength of 850 nm was placed at the center of the gap to excite SPP waveguide modes. The symmetric SPP waveguide mode is then excited by the *z*-directional electric dipole and propagates on the top surface of the waveguide, showing strong electric field confinement (Figure 4A,B). Next, to examine the scattered light intensity distribution of the SPP waveguide mode at the tapered end of the double-strip waveguide, we calculated the time-averaged distribution of the

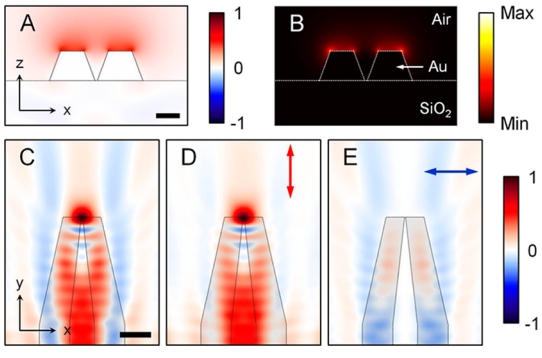

Figure 4. Calculated field profiles of the symmetric SPP waveguide mode excited in the double-strip plasmonic waveguide. (A) The *z*-component of the electric field profile and (B) the electric field intensity distribution of the symmetric SPP waveguide mode. The scale bar in (A) is 300 nm. (C–E) The *z*-components of (C) total and (D, E) polarization-resolved time-averaged Poynting vector distributions of the symmetric SPP waveguide mode. These distributions were obtained at a position 400 nm above the top surface of the waveguide. The scale bar in (C) is 1 μm.

dx.doi.org/10.1021/nl3044822 | *Nano Lett.* 2013, 13, 772–776

z-component of the Poynting vector at a position 400 nm above the top surface (Figure 4C). The simulation shows that the symmetric SPP waveguide mode was scattered at the end of the waveguide and focused strongly above the waveguide. The fwhm size of this focused light spot is estimated to be 660 nm. Since the electric fields of the symmetric SPP waveguide mode are oriented normal to the top surfaces of the gold strips (Figure 4A), the polarization direction of the focused light spot should be parallel to the waveguide axis, which was confirmed by FDTD simulations (Figure 4D,E). All these simulation results remarkably agreed with the total and polarization-resolved EL images of Figure 3A,D. In particular, the measured and calculated sizes of the focused spot are in excellent agreement. Therefore, we can conclude that the light emission from the NW LED was coupled to the symmetric SPP waveguide mode, and as a result, the subwavelength-sized focused spot was observed in the experiment. Although two antisymmetric SPP waveguide modes also exist in the double-strip plasmonic waveguide, as shown in the calculated dispersion curves (Figure S3), the focused emission patterns at the end of the waveguide are not observed for these modes (Figure S4).

Lastly, we calculated the coupling efficiency between the NW LED and the plasmonic waveguide using FDTD simulation. In the simulation, a 2.3 μm long NW with a triangular cross section was introduced at the center of the air gap of the double-strip waveguide with an infinite length to the right (Figure 5A). The structural parameters of the waveguide

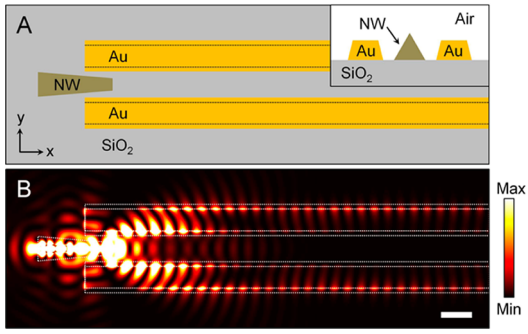

Figure 5. FDTD simulation of the light coupling from the NW LED to the double-strip plasmonic waveguide. (A) Calculation structure including the NW placed on SiO_2 substrate and at the center of the two straight gold strips. The NW has a triangular cross section and a length of 2.3 μm, and one side lengths on the left and right cross sections of the NW are 700 and 400 nm, respectively. The inset shows the cross-sectional view of the coupling region of the NW and waveguide, where the waveguide has a trapezoidal cross section and a thickness of 400 nm. The tapered termination of the waveguide is unnecessary to calculate coupling efficiency. (B) Calculated electric field intensity distribution on the top surface of the waveguide. A single dipole source was introduced at the center of the NW, and the light emission from the NW was coupled to the symmetric SPP waveguide mode. The scale bar is 1 μm.

identical to those in Figure 1B were used, such as trapezoidal cross section, thickness of 400 nm, and width of 1000 nm. A single dipole source with a wavelength of 850 nm was introduced inside the NW to excite a NW cavity mode, which can be coupled to the symmetric SPP waveguide mode. To estimate the efficiency of converting the light emitted from the NW into the symmetric SPP waveguide mode, we calculated the total power emitted from the NW, P_{NW}, and the transmitted power of the waveguide mode at different detection positions along the waveguide axis, P_{trans}. By plotting and fitting the values of P_{trans}/P_{NW} as a function of the detection position,[7] the coupling efficiency can be calculated (Figure S5). In the structure of Figure 5A, the propagation length of the symmetric SPP waveguide mode was ~10.6 μm, and the coupling efficiency was estimated to be ~1.6%. In addition, the electrical field intensity distribution was obtained just above the top surface of the waveguide (Figure 5B). It is observed that the emitted light from the NW is symmetrically coupled to the SPP waveguide mode and propagates on the top surface of the waveguide. We note that the relatively low coupling efficiency can be improved by optimization of the position of the NW and the shape of the waveguide in the coupling region.[19,22] For example, FDTD simulation showed that the coupling efficiency was increased to ~2.8% by reducing the thickness of the gold layer in the plasmonic waveguide (Figure S6).

In summary, we have demonstrated a double-strip plasmonic waveguide integrated with an electrically driven GaAs NW LED. The NW with an axial p/n junction was used as an internal light source of the plasmonic waveguide and operated by current injection. In measurements of the polarization-resolved images and spectra, we observed the light coupling from the NW LED to the plasmonic waveguide and the propagation of a SPP waveguide mode. The guided SPP mode was focused with a subwavelength size of ~600 nm by adiabatically reducing the gap and width of the double-strip waveguide. In FDTD simulation, the time-averaged Poynting vector distributions effectively reproduced the measured polarization-resolved EL images and focused light spot yielded by the symmetric SPP waveguide mode. We believe that our integrated plasmonic device is simple and practical and thus widely applicable to research fields requiring various functionalities, such as biochemical sensing and quantum information.

■ ASSOCIATED CONTENT

Supporting Information

Additional information and figures. This material is available free of charge via the Internet at http://pubs.acs.org.

■ AUTHOR INFORMATION

Corresponding Author

*E-mail hgpark@korea.ac.kr.

Notes

The authors declare no competing financial interest.

■ ACKNOWLEDGMENTS

This work was supported by the National Research Foundation of Korea (NRF) grant funded by the Korea government (MEST) (No. 2012-0000242). Y.-S.N. acknowledges the support of this work by the TJ Park Science Fellowship.

■ REFERENCES

(1) Oulton, R. F.; Sorger, V. J.; Zentgraf, T.; Ma, R.-M.; Gladden, C.; Dai, L.; Bartal, G.; Zhang, X. *Nature* **2009**, *461*, 629−632.

(2) Kang, J.-H.; Kim, K.; Ee, H.-S.; Lee, Y.-H.; Yoon, T.-Y.; Seo, M.-K.; Park, H.-G. *Nat. Commun.* **2011**, *2*, 582 DOI: 10.1038/ncomms1592.

(3) Hill, M. T.; Marell, M.; Leong, E. S. P.; Smalbrugge, B.; Zhu, Y.; Sun, M.; Veldhoven, P. J.; Geluk, E. J.; Karouta, F.; Oei, Y.-S.; Nötzel, R.; Ning, C.-Z.; Smit, M. K. *Opt. Express* **2009**, *17*, 11107−11112.

(4) Kwon, S.-H.; Kang, J.-H.; Seassal, C.; Kim, S.-K.; Regreny, P.; Lee, Y.-H.; Lieber, C. M.; Park, H.-G. *Nano Lett.* **2010**, *10*, 3679−3683.
(5) Khajavikhan, M.; Simic, A.; Katz, M.; Lee, J. H.; Slutsky, B.; Mizrahi, A.; Lomakin, V.; Fainman, Y. *Nature* **2012**, *482*, 204−207.
(6) Gramotnev, D. K.; Bozhevolnyi, S. I. *Nat. Photonics* **2010**, *4*, 83−91.
(7) Gramotnev, D. K.; Nielsen, M. G.; Tan, S. J.; Kurth, M. L.; Bozhevolnyi, S. I. *Nano Lett.* **2012**, *12*, 359−363.
(8) Sorger, V. J.; Ye, Z.; Oulton, R. F.; Wang, Y.; Bartal, G.; Yin, X.; Zhang, X. *Nat. Commun.* **2011**, *2*, 331 DOI: 10.1038/ncomms1315.
(9) Krenn, J. R.; Lamprecht, B.; Ditlbacher, H.; Schider, G.; Salerno, M.; Leitner, A.; Aussenegg, F. R. *Europhys. Lett.* **2002**, *60*, 663−669.
(10) Zia, R.; Schuller, J. A.; Brongersma, M. L. *Phys. Rev. B* **2006**, *74*, 165415.
(11) Bozhevolnyi, S. I.; Volkov, V. S.; Devaux, E.; Laluet, J.-Y.; Ebbesen, T. W. *Nature* **2006**, *440*, 508−511.
(12) Volkov, V. S.; Bozhevolnyi, S. I.; Rodrigo, S. G.; Martin-Moreno, L.; Garcia-Vidal, F. J.; Devaux, E.; Ebbesen, T. W. *Nano Lett.* **2009**, *9*, 1278−1282.
(13) Veronis, G.; Fan, S. *Opt. Lett.* **2005**, *30*, 3359−3361.
(14) Pile, D. F. P.; Gramotnev, D. K.; Oulton, R. F.; Zhang, X. *Opt. Express* **2007**, *15*, 13669−13674.
(15) Walters, R. J.; van Loon, R. V. A.; Brunets, I.; Schmitz, J.; Polman, A. *Nat. Mater.* **2010**, *9*, 21−25.
(16) Babuty, A.; Bousseksou, A.; Tetienne, J.-P.; Doyen, I. M.; Sirtori, C.; Beaudoin, G.; Sagnes, I.; Wilde, Y. D.; Colombelli, R. *Phys. Rev. Lett.* **2010**, *104*, 226806.
(17) Koller, D. M.; Hohenau, A.; Ditlbacher, H.; Galler, N.; Reil, F.; Aussenegg, F. R.; Leitner, A.; List, E. J. W.; Krenn, J. R. *Nat. Photonics* **2008**, *2*, 684−687.
(18) Fan, P.; Colombo, C.; Huang, K. C. Y.; Krogstrup, P.; Nygard, J.; Fontcuberta i Morral, A.; Brongersma, M. L. *Nano Lett.* **2012**, *12*, 4943−4947.
(19) Schnell, M.; Alonso-Gonzalez, P.; Arzubiaga, L.; Casanova, F.; Hueso, L. E.; Chuvilin, A.; Hillenbrand, R. *Nat. Photonics* **2011**, *5*, 283−287.
(20) Kawata, S.; Inouye, Y.; Verma, P. *Nat. Photonics* **2009**, *3*, 388−394.
(21) Gramotnev, D. K. *J. Appl. Phys.* **2005**, *98*, 104302.
(22) Pile, D. F.; Gramotnev, D. K. *Appl. Phys. Lett.* **2006**, *89*, 041111.
(23) Gradecak, S.; Qian, F.; Li, Y.; Park, H.-G.; Lieber, C. M. *Appl. Phys. Lett.* **2005**, *87*, 173111.
(24) Qian, F.; Li, Y.; Gradecak, S.; Park, H.-G.; Dong, Y.; Ding, Y.; Wang, Z. L.; Lieber, C. M. *Nat. Mater.* **2008**, *7*, 701−706.
(25) Seo, M.-K.; Yang, J.-K.; Jeong, K.-Y.; Park, H.-G.; Qian, F.; Ee, H.-S.; No, Y.-S.; Lee, Y.-H. *Nano Lett.* **2008**, *8*, 4534−4538.